Chapter 2
Design of Fuel Cells and Reactors, Estimation of Process Parameters, Their Modelling and Optimization

2.1 Introduction

Fuel cell systems are a promising alternative power source based technologies that are vastly used in today's industrial applications. Fuel cells are clean, quiet, and feasible devices that transformed chemical changes into electricity to be utilized. They are operational and can generate fuel as long as it is supplied with oxygen and hydrocarbons. Evidently, emission such as carbon dioxide are greatly reduced mainly by fuel cell technologies compared to conventional technologies (Höök and Aleklett 2010). Besides, fuel cells are ideal for power generation to provide supplemental power and backup assurance for critical areas, or for on-site service in areas that are inaccessible by power lines. Since fuel cells operate silently, they reduce noise pollution as well as air pollution and the waste heat from a fuel cell can be used to provide hot water or space heating. Fuel cells are the best alternative because they combine higher fuel efficiency with low or no pollution, greater flexibility in installation and operation, quiet operation, low vibration, and potentially lower maintenance and capital costs (Stambouli and Traversa 2002). The wide range of applications includes unmanned under water vehicle, automotive, locomotives, surface ships, electronic component and automobiles (Woodland 2001). Fuel cells are a propitious alternative energy conversion technology. Typical fuel cell utilizes hydrogen as a fuel and reacting it with oxygen to produce electricity. The fundamental fabrication of these fuel cells is its ability to employ the equations of standard reactor design to the reaction kinetics of a fuel cell as shown below (Figs. 2.1 and 2.2).

$$\textit{Anode}: \mathrm{H_2} + \mathrm{O^{2-}} \rightarrow \mathrm{H_2O} + 2\mathrm{e^-}$$

$$\textit{Cathode}: \frac{1}{2}\mathrm{O_2} + 2\mathrm{e^-} \rightarrow \mathrm{O^{2-}}$$

$$\textit{Overall}: \mathrm{H_2} + \frac{1}{2}\mathrm{O_2} \rightarrow \mathrm{H_2O}$$

S. Bagheri, *Catalysis for Green Energy and Technology*,
Green Energy and Technology, DOI 10.1007/978-3-319-43104-8_2

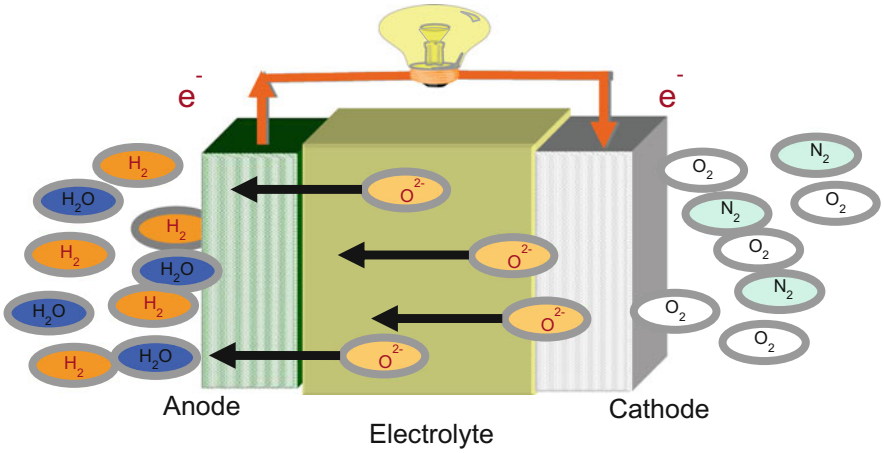

Fig. 2.1 Reactions of a typical fuel cell

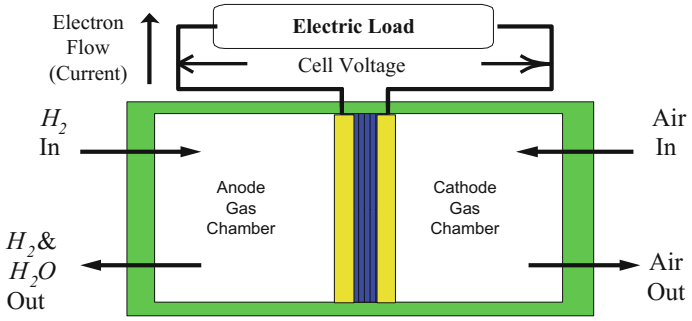

Fig. 2.2 Flow diagram for a fuel cell system

In this reaction, when each mole of hydrogen used up, two moles of electrons moved through the electric load. Conversion of electron flow can be done by applying Faraday's constant ($F = 96{,}485$ coulombs/mole of electrons) and mathematical calculation of energy utilizes. The potential of a fuel cell usually relates in terms of efficiency, of the energy available from the reaction in the fuel cell system. A recent study in polymer electrolyte membrane (PEM) and catalyst technology have increased the fuel cell power density and made them available for automobiles and portable power applications, as well in power plants. The negative potential side of the cell stack is fed by the fuel processing system (FPS) which convert natural gas or other hydrocarbons into clean, purity and rich hydrogen and by-products. On the other hand, the positive potential is supplied with oxygen gas. Both gases in anode and cathode reacts electrochemically with each other to generate electricity.

2.2 Drawback in Fuel Cell Power Systems

The most complication in fuel cell power systems lies within the FPS to the anode site of the cell stack. Poor supply of oxygen causes "starvation" of the cell, which denotes that the platinum catalyst will start consuming the graphite used in the flow fields, thus resulting in fast and permanent harm (Ahn 2011; Mandal 2016; Chen and Hsu 2011). While insufficient supply of oxygen reduces the cell span life, too much hydrogen output from FPS lowers its efficiency, which is not promising. This is due to a high fuel flow in a substantial surplus of hydrogen, leaving the fuel cell results in a relatively high reformer temperature with high conversion efficiency, but with lower overall plant efficiency. This causes are resulted from excess amounts of hydrogen being burned rather than utilized in the conversion to electricity (Scheffler 1991). Another problem with fuel cells, especially PEM is to maintain the carbon monoxide level below a critical limit 10 ppm for PEM fuel cells (Ormerod 2003; Schmittinger and Vahidi 2008; Pettersson and Westerholm 2001). Carbon monoxide is harmful and easily produced during the reforming reaction, resulting in de-activation of the platinum electro catalyst. In the worst scenario, occurrence of carbon monoxide limits hydrogen from reacting in the anode side influencing the system efficiency and lowers the fuel cell voltage measurement.

Another crucial limitation is in the temperature of CPO, where it must be at a certain point (Linde 1983). Too high temperature damages CPO catalyst bed permanently while the temperature decreases lower down the fuel reaction rate (Landsman 1989). Not only that, the implementation of these designs is the absence of reliable measurements of hydrogen partial pressure in the cell stack. Existing sensors are not apt for use with these controllers because, as discussed, commercially available sensors are not fabricated to operate in a reformate gas environment. This is because the sensors are either too bulky or costly. Sensors that are affordable are not reliable or do not have long life time (Chong and Kumar 2003).

2.3 Design of Fuel Cells and Reactors

In a fuel system, generating chemical energy into electrical energy can be done by transforming hydrogen and oxygen into steam were restricted by efficiency limits of the Carnot thermal cycle (Larminie and Dicks 2000). Since then, many remarkable approaches have been investigated on fuel cell technology; however, it is not widely used in the automotive industry. This is because the impotent efficiency of the hydrogen distribution centre in the fuel cell system (Lovins and Williams 1999) as well as the trouble related to storing hydrogen on board an automobile. Thus, designing a fuel cell that employs carbon-based hydrogenous fuel are utilized as it widely available, aids in generating an in situ hydrogen and enables easy store on-board a vehicle (Dicks 1996).

The main components of a fuel cell power system comprise of two units that are the fuel cell stack and the auxiliary subsystem. In this context, the fuel cell stack is discussed as the core design which comprises of a reformer unit, a water shift gas reactor and a catalytic preferential oxidation reactor, which converts methane gas into hydrogen of the desired purity as shown in Fig. 2.3. This concept employs in a model of a polymer electrolyte membrane (PEM) fuel cell system and the quantity of power induced is reckoned as a function of hydrogen penetrating the fuel cell. Subsequently, the hydrogen penetrates into the fuel cell and intermingle with oxygen to promote electrical power which pilot an electric motor. However, in designing an ideal fuel cell, numerous operational constraints are to be taken note of such as the steam or autothermal reforming, water gas shift (WGS) reactor and catalytic preferential oxidation (PrOx) reactor.

The reforming process function as cleaning of sulfur from natural hydrocarbon to avoid fuel cell anode electrode bane. Then, the steam reforming of methane enters the WGS reactor, which was designed as a packed bed plug flow reactor to inhibit all exothermic reactors. When the temperature is high, the preliminary reaction rate is rapid but the equilibrium conversion is low. On the other hand, when the temperature is low, the reaction rate decreases; however, the equilibrium conversion is high. Therefore, water gas shift reactor is typically split into two zones with a high temperature zone (where the rate of reaction is low) and a lower temperature zone (where the rate of reaction is high). Following, is the catalytic preferential oxidation (PrOx) reactor, which was designed as an isothermal packed bed reactor to avoid poisoning of the PEM system from the output of water gas shift reactor due to carbon monoxide gas (Godat and Marechal 2003).

Lastly, the effect of manipulating the feed rate of methane on the overall hydrogen generated with the same reactor train was scrutinized. The methane supplied to the reformer differ between 0.0163 and 0.167 mol/s. The steam flow rate was calibrated in order to maintain the steam to methane ratio at 3:1 for all studies. The correlation between hydrogen egress from the catalytic partial oxidation reactor and the methane infiltrate into the reformer is as shown in Eq. 2.1.

$$N_{\cdot H_2} = 3.12 N_{\cdot CH_4} \tag{2.1}$$

From Eq. 2.1, a fitting straight line can be plotted in a steady state of hydrogen production rate against the methane production is represented in Fig. 2.4. This result displayed that the ideal fuel cell can be operated near to equilibrium.

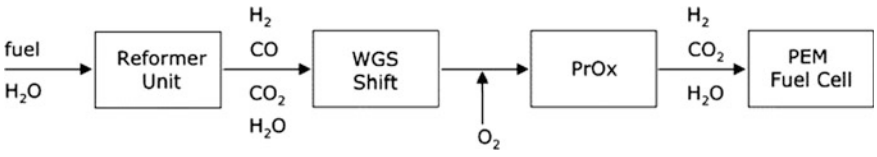

Fig. 2.3 A simple designated fuel cell power system (Zalc et al. 2002)

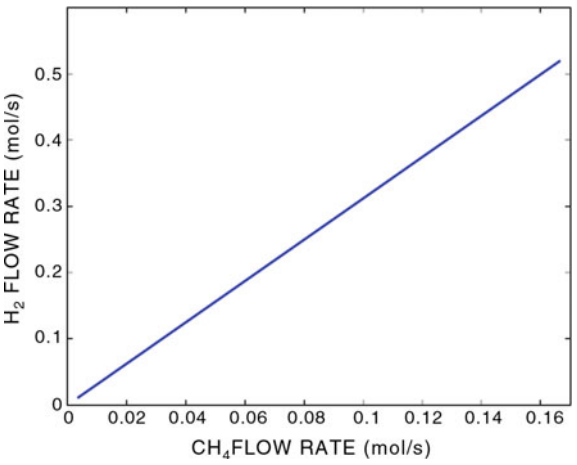

Fig. 2.4 A fitting straight line can be plotted in steady state of hydrogen production rate against the methane production (Bordo and Murshid 2006)

2.4 Estimation of Process Parameters in Fuel Cells

One of the main limitation of the fuel cell is its cost, efficiency, size and maintaining the auxiliary part in order to sustain the physical properties of fuels. The modelling of a prototype fuel cell is typically associated with the reactor operation to the system parameters, such as, concentrations of the reactant, loading of the catalyst, pressure, temperature, and etc. On the other hand, temperature, pressure, flow rate, composition, and geometry are coordinated with heat and mass transfer. The mathematical association between the parameters and unknown are the prime constituent in providing the estimation optimum performance information in engineering the fuel cell system.

One of the parameters to be taken note are the water dynamics in the fuel cell stack (Kazmi and Bhatti 2012). Water dynamics play a role as it comprises of electro-osmosis flow from the negatively charged electrode to the positively charged electrode and diffuse back to and fro across the membrane as shown in Fig. 2.5.

This is because the existence of water contents of the stack is vulnerable to length of membrane life, cold environment, proton conductivity and reactant gas transportation. For instance, in a cold environment, the water content in the stack can interchange phase due to subfreezing temperature. Besides, lacking or too much of water in the stack can greatly decline the performance of the system. When the amount of water is less, it can cause the membrane to dry up and this would form cracks in the membrane which eventually resulted in a reduction in the performance and short life span of the system. In the latter part, too much water in the stack prompt to flooding the pores of the porous gas diffusion layer and advert the dispersal of the reactants to the catalyst. Subsequently, the produced water at the positive electrode diffuses into the negative electrode due to the gradient of water concentration. This resulted in severe problems where water will be accumulated

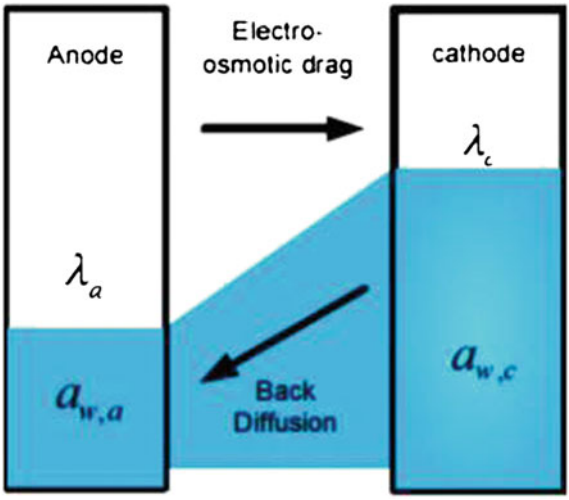

Fig. 2.5 Adapted from (Kazmi and Bhatti 2012)

and obstruct the sufficient dispersal of fuel gas. In addition, other dynamical behaviour such as listed below (A-G) are evaluated and adequately modelled to ensure the quality of fuel needed by fuel cells.

(A) Cell Reversible Voltage (E_{oc})

The ideal reversible/open circuit voltage for a fuel cell is defined as electrical work done in moving per unit charge on one mole of electrons through the fuel cell circuit in Eq. 2.2.

$$E_{OC} = W_{el}/2F \tag{2.2}$$

where, F is the Faraday constant, W_{el} is the electrical work and "2" in the denominator denotes the number of electrons that flow for one mole of hydrogen. In an ideal system, it is derived from an alteration of Nernst equations assessing from the feasible variations of temperature from the standard value of 25 °C.

$$E_{Nerst} = 1.229 - 0.85^{10^{-3}}(T - 298.15) + 4.31^{10^{-5}}T[\ln(P_{H_2}) + 1/2\ln(P_{O_2}) \tag{2.3}$$

whereby T is the temperature of cell operation in [K], P_{H2} and P_{O2} are respectively the partial pressures of hydrogen and oxygen in [atm].

(B) Coefficient of Fuel Utilization (μF)

In experimental, hydrogen that enters the fuel cell is not entirely used in the electrochemical reaction. Therefore, the fuel utilization coefficient, μF, is as shown in Eq. 2.4 below:

$$\mu F = \text{Mass of fuel reacted in cell/Mass of fuel input to cell} \tag{2.4}$$

The mass of fuel responded in the fuel cell is ameliorate with high fuel percentage of hydrogen (Ralph et al. 1997).

(C) Efficiency of Fuel Cell (η):

The fuel cell efficiency is influenced by the actual voltage produced in the fuel cell. V_{out}, the actual fuel cell output voltage, are as in Eq. 2.5.

$$V_{out} = E_{oc} - V_{drop} \tag{2.5}$$

where, V_{drop} is, the voltage drop within the fuel cell. The cell efficiency η is then written as in Eq. 2.6:

$$\eta = (\mu F\ VC)/E_{oc} \tag{2.6}$$

whereby the voltage drop in the system is predominantly due to polarization losses, which involves activation polarization, concentration polarization and losses of ohmic polarization (Gür et al. 1980).

(D) Consumption of Hydrogen

The hydrogen consumption in a fuel cell is determined by the type of fuel cell and the concentration of hydrogen at standard temperature and pressure as in Eq. 2.7 below.

$$H_2\, consumption = \left(2.02 \times 10^{-3} P_{out}\right)/(2V_c F) \tag{2.7}$$

whereby 2.02×10^{-3} kg/mole is the molar mass of hydrogen at STP and P_{out} is the electrical power output of the fuel cell.

(E) Heating Rate of Fuel Cell

The ideal E_{oc} is produced only if the whole heat energy of combustion in the fuel cell is transformed into electrical energy. However, in practical, some heat energy may have lost in the by products that caused from the electrochemical reactions at the positive and negative electrode. Thus, by using the net heat produced during combustion (LHV) value, the E_{oc} for a fuel cell is 1.25 V (Gomaton and Jewell 2003).

$$Heating\ rate = nI(1.25 - V_c)W \tag{2.8}$$

whereby I, is the maximum current for a stack of n cells.

(F) Net Power Output (NP_{out})

The net power output (NP_{out}) of fuel cell is the available electric power output to the connected load. The net power output is equivalent to the electrical power output

P_{out} deducted the total parasitic power and conversion losses. The subsystems in a fuel cell unit rely on the operating temperature range, the type of the fuel cell, and the nature of electrochemical reactions at both terminal electrode with the Eq. 2.9 as below.

$$NP_{out} = P_{out} - \sum(\text{parasitic loss} + \text{conversion loss}) \tag{2.9}$$

(G) Total Efficiency (η tot)

The total efficiency of the fuel cell generator system, η tot, is the ratio of the total net power output and the net heat released in the exhaust to the total system of net heat production during combustion of the fuel input as written Eq. 2.10:

$$\eta\,\text{tot} = (NP_{out} + H_{exh})/T_{LHV} \tag{2.10}$$

whereby H_{exh} is the net heat released in the exhaust and T_{LHV} is the total system LHV fuel input.

2.5 Modelling and Optimization for Fuel Cells

There are two distinct methods in modelling and optimizing the fuel stack cell; by static or dynamic behaviour. The latter modelling, which applies Spiros stack model shows that understanding the dynamic behaviour is the key to the fuel cell system in the time domain to the changing of the load. Spiros' model utilizes large mass of loads with uniform environment inside the reactors making the assumption sensible due to the exit values of mole fractions of interest. However, accuracy of mass models can be greatly influenced by thermal waves and reaction zones which may cause variability in modelling model and inscribed with rigidity of the tools. Thus, the parameters such as the catalytic partial oxidation, water gas shift and catalytic preferential oxidation in the irreversibility of the fuel stack cell needed extended measurements.

2.5.1 Catalytic Partial Oxidation (CPO)

In the CPO, there are two main reactions that plays major role:

(i) $$\textit{Partial Oxidation}\,(Pox)\text{: } CH_4 + 1/2O_2 \rightarrow CO + 2H_2 \tag{2.11}$$

(ii) $$\textit{Full Oxidation}\,(Fox)\text{: } CH_4 + 2O_2 \rightarrow CO_2 + 2H_2O \tag{2.12}$$

In partial oxidation, it generates essential hydrogen gases, but also carbon monoxide, which prompts to poisoning in the cell stack. On the other hand, full

oxidation occurs by supplying additional heat to the system which generates the feasibility of a partial oxidation reaction. The rate of reaction for full-and partial-oxidation are depicted in the Equation below:

$$Rate\ of\ Pox = vrt \tag{2.13}$$

$$Rate\ of\ Fox = (1 - v)rt \tag{2.14}$$

where, v is a selectivity variable (Dicks 1996; Ormerod 2003) which are influenced by a ration of air-fuel and rt is the summation of reaction rate shown in Eq. 2.15:

$$rt = kg[\mathrm{O_2}]\frac{[\mathrm{CH_4}]}{[\mathrm{CH_4}] + \varepsilon} \tag{2.15}$$

whereby $[O_2]$ and $[CH_4]$ indicates the concentrations of oxygen and methane and kg and ε are coefficients from empirical studies. The term, kg$[O_2]$, in Eq. 2.15 denotes the mass transfer rate of oxygen from gas phase to the catalyst. The second term, $[CH_4]/[CH_4] + \varepsilon$ is a function that reckons for the position in which methane is the limiting reactant.

The dynamic model is derived from mole balance equations as shown below

$$M = u_f + u_a - F_{out}^{CPO} + l_1 r_{P_{ox}} V + l_2 r_{F_{ox}} V \tag{2.16}$$

where, u_f, u_a and F_{out}^{CPO} (mole/sec) are the fuel, air and exit molar flow vectors, V is the reactor volume in meter per cubic, and l_1 and l_2 are stoichiometric coefficient vectors where;

$$l_1 = [0 \quad -1 \quad 1 \quad 0 \quad 2 \quad -1/2] \tag{2.17}$$

$$l_2 = [0 \quad -1 \quad 0 \quad 1 \quad 0 \quad 2 \quad -2] \tag{2.18}$$

Thus, the energy balance principle of dynamics given temperature T is as shown in Eq. 2.19.

$$\left(m_{c_p}\right)T - u_f h\left(T_f\right) + u_a h(T_a) - F_{out}^{CPO} hT + \delta H_{Pox} r_{Pox} V + \delta H_{Fox} r_{Fox} V \tag{2.19}$$

whereby T is the reaction temperature in Kelvin, m is the mass in kg, cp (kJ/kg K) a is the specific heat capacity of the catalyst bed. The terms $h(T_f)$, $h(T_a)$ and h(T) are the molar enthalpies of ideal gas for fuel, air and the exit temperatures respectively and δ H is the reaction heat at reference temperature.

2.5.2 Water Gas Shift (WGS)

This system comprises of two inlet streams in which (1) hydrocarbon reforming from CPO and (2) feed from the reservoir. In the reactor carbon monoxide reacts with water and generates hydrogen and carbon dioxide. Thus, an expression on rate of reaction for WGS, from the principle of Mass Action Law and the Arrhenius Equation is expressed in Eq. 2.20.

$$r = M_f e^{\frac{K_f}{RT}}[\mathrm{CO}][\mathrm{H_2O}] - M_b e^{\frac{K_b}{RT}}[\mathrm{CO_2}][\mathrm{H_2}] \tag{2.20}$$

where, M_f, M_b, K_f and K_b are parameters of the reaction rate.

Conveying it in terms of expressing the mole balance equations, M, below is as in Eq. 2.21:

$$M = u_g + u_w - F_{out}^{WGS} + krV \tag{2.21}$$

whereby u_g and u_w, are the flow vectors of gas, air and F_{out}^{WGS} is the exit molar flow vectors and q is a constant with [0 0 −1 1 1 −1 0].

Subsequently, the dynamics of the temperature T are equated as below:

$$(m_{cp})T = u_g h(T_g) + u_w h(T_w) - F_{out}^{WGS} h(T) + \delta H_r V \tag{2.22}$$

Inscribe that the dynamic variables, M and T and constants, V, m, cp and δ H have been used in the reactor system CPO, WGS and PrOx as expressed.

2.5.3 Catalytic Preferential Oxidation (PrOx)

The PrOx is the last stage in eliminating poisonous carbon monoxide such as proton exchange membrane in fuel cell into carbon dioxide and water as expressed in Eqs. 2.23 and 2.24

$$\mathrm{CO} + 1/2\,\mathrm{O_2} \rightarrow \mathrm{CO_2} \tag{2.23}$$

$$\mathrm{H_2} + 1/2\mathrm{O_2} \rightarrow \mathrm{H_2O} \tag{2.24}$$

Apt expressions of the rate of reaction are expressed in equations below,

$$r_{\mathrm{CO}} = s^{PrOx} r_t^{PrOx} \tag{2.25}$$

$$r_{\mathrm{H_2}} = (1 - s^{PrOx}) r_t^{Prox} \tag{2.26}$$

where, s^{PrOx} s is a selectivity variable. Therefore, the total rate of reaction can be equated as:

$$r_t^{PrOx} = k[\mathrm{CO}][\mathrm{O_2}]^{1/2} \tag{2.27}$$

Then,

$$M = u_g^{PrOx} + u_a^{PrOx} - F_{out}^{PrOx} + m_1^{PrOx} r_{\mathrm{CO}} V + m_2^{PrOx} r_{\mathrm{H_2}} V \tag{2.28}$$

where, $u_g^{PrOx}, u_a^{PrOx},$. and F_{out}^{PrOx} are the molar flow vectors for gas, air and exit respectively, and given, m_1^{PrOx} = [0 0 −1 1 0 0 −1/2] and m_2^{PrOX} = [0 0 0 0 −1 1 −1/2].

Similarly, temperature dynamics are given by

$$\left(mc_p\right)T = u_g^{PrOx} k\left(T_g\right) + u_a^{PrOx} k(T_a) - F_{out}^{PrOx} h(T) + \delta H_{\mathrm{CO}} r_{\mathrm{CO}} V + \delta H_{\mathrm{H_2}} r_{\mathrm{H_2}} V \tag{2.29}$$

References

Ahn J-W (2011) Control and analysis of air, water, and thermal systems for a polymer electrolyte membrane fuel cell. Auburn University, Alabama

Bordo MD, Murshid AP (2006) Globalization and changing patterns in the international transmission of shocks in financial markets. J Int Money Finance 25(4):655–674

Chen Z, Hsu R (2011) Catalyst support degradation. In: PEM fuel cell failure mode analysis. CRC Press, Boca Raton, pp 33–72

Chong C-Y, Kumar SP (2003) Sensor networks: evolution, opportunities, and challenges. Proc IEEE 91(8):1247–1256

Dicks AL (1996) Hydrogen generation from natural gas for the fuel cell systems of tomorrow. J Pow Sources 61(1–2):113–124

Godat J, Marechal F (2003) Optimization of a fuel cell system using process integration techniques. J Pow Sources 118(1):411–423

Gomaton P, Jewell W (2003) Fuel parameter and quality constraints for fuel cell distributed generators. In: 2003 IEEE PES transmission and distribution conference and exposition. IEEE, pp 409–412

Gür TM, Raistrick ID, Huggins RA (1980) Steady-State D-C Polarization Characteristics of the O_2, Pt/Stabilized Zirconia Interface. J Electrochem Soc 127(12):2620–2628

Höök M, Aleklett K (2010) A review on coal-to-liquid fuels and its coal consumption. Int J Energy Res 34(10):848–864

Kazmi IH, Bhatti AI (2012) Parameter estimation of proton exchange membrane fuel cell system using sliding mode observer. Int J Innovative Comput Inform Control 8(7B):5137–5148

Landsman N (1989) Limitations to dimensional reduction at high temperature. Nucl Phys B 322 (2):498–530

Larminie J, Dicks A (2000) Fuel Systems Explained. Wiley, Chichester

Linde AD (1983) Decay of the false vacuum at finite temperature. Nucl Phys B 216(2):421–445

Lovins AB, Williams BD (1999) A strategy for the hydrogen transition. Rocky Mountain Institute Snowmass, Colorado

Mandal P (2016) Investigation and mitigation of degradation in hydrogen fuel cells
Ormerod RM (2003) Solid oxide fuel cells. Chem Soc Rev 32(1):17–28
Pettersson LJ, Westerholm R (2001) State of the art of multi-fuel reformers for fuel cell vehicles: problem identification and research needs. Int J Hydrogen Energy 26(3):243–264
Ralph T, Hards G, Keating J, Campbell S, Wilkinson D, Davis M, St-Pierre J, Johnson M (1997) Low cost electrodes for proton exchange membrane fuel cells performance in single cells and Ballard stacks. J Electrochem Soc 144(11):3845–3857
Scheffler GW (1991) Fuel cell power plant fuel control. Google Patents
Schmittinger W, Vahidi A (2008) A review of the main parameters influencing long-term performance and durability of PEM fuel cells. J Pow Sources 180(1):1–14
Stambouli AB, Traversa E (2002) Solid oxide fuel cells (SOFCs): a review of an environmentally clean and efficient source of energy. Renew Sustainable Energy Rev 6(5):433–455
Woodland RLK (2001) Autonomous marine vehicle. Google Patents
Zalc J, Sokolovskii V, Löffler D (2002) Are noble metal-based water–gas shift catalysts practical for automotive fuel processing? J Catalysis 206(1):169–171

http://www.springer.com/978-3-319-43103-1

Catalysis for Green Energy and Technology
Bagheri, S.
2017, VIII, 207 p. 31 illus., Hardcover
ISBN: 978-3-319-43103-1